Author/s:
Olusa, TAO;Ismail, SMY;Murray, CM;Davies, HMS

Title:
Radiographic assessment of carpal conformation in the horse: Technique development and validation of the consistency of measurements

Date:
2021-03

Citation:
Olusa, T. A. O., Ismail, S. M. Y., Murray, C. M. & Davies, H. M. S. (2021). Radiographic assessment of carpal conformation in the horse: Technique development and validation of the consistency of measurements. Anatomia, Histologia, Embryologia: journal of veterinary medicine series C, 50 (2), pp.284-299. https://doi.org/10.1111/ahe.12627.

Persistent Link:
https://hdl.handle.net/11343/276577

DR. TIMOTHY AKINBOWALE OLUSA (Orcid ID : 0000-0001-9853-4788)

Article type : Original Article

ORIGINAL ARTICLE

Title: RADIOGRAPHIC ASSESSMENT OF CARPAL CONFORMATION IN THE HORSE: TECHNIQUE DEVELOPMENT AND VALIDATION OF THE CONSISTENCY OF MEASUREMENTS

Running head: OBJECTIVE EVALUATION OF THE EQUINE CARPUS

Authors: Timothy, A.O. Olusa[1]*; Sa'ad, M.Y. Ismail[1]; Christina, M. Murray[1] & Helen, M.S. Davies[1]

Institution affiliations: [1]Faculty of Veterinary and Agricultural Sciences, University of Melbourne, Werribee VIC 3030, Australia

*Corresponding author: Timothy A.O. Olusa,
Faculty of Veterinary and Agricultural Sciences,
University of Melbourne, Werribee VIC 3030, Australia
E-mail: timolusa1@gmail.com & olusat@unimelb.edu.au

This is the author manuscript accepted for publication and has undergone full peer review but has not been through the copyediting, typesetting, pagination and proofreading process, which may lead to differences between this version and the Version of Record. Please cite this article as doi: 10.1111/AHE.12627

ABSTRACT

Carpal conformation is often considered as a contributory factor to performance and lameness in the horse; however, few attempts have been made to objectively measure radiographic variations of carpal conformation in horses due to insufficient measurable carpal parameters. This pilot study used carpal radiographic images acquired from 10 cadaveric equine forelimbs transected at the antebrachial midshaft from 7 adult horses (7.2±2.6 years), positioned at "zero lateromedial" (ZLM) and "zero dorsopalmar" (ZDP) views, to investigate the anatomy of the equine carpus and develop parameters that could be objectively used to assess carpal conformation in horses.

Dorsal carpal angle (DCA: 176.61±0.66º), distal radial slope carpal angle (DRSCA: 145.59±2.19º), intermediate carpal bone proximal tuberosity-radial angle (CiPxTRA: 115.69±3.15º) and third carpal bone palmar facet angle (C3PalFCA: 84.43±1.13º) were all developed from the ZLM view while medial carpal angle (MCA: 183.34±1.02º), disto-dorsal slope angle of the third carpal bone (C3DDSA: 8.27±0.92º) and width ratio of distal radius to proximal metacarpus (WDR:WPM = 1.13±.03) were 3 of the 10 parameters developed from the ZDP view.

Easy to identify and measurable parameters will help to provide quantitative assessment of carpal conformation in the horse with potential of eliminating subjective observational variation errors between clinicians. These newly developed parameters will be useful in further studies to measure variations in the conformation of the equine carpus in live horses and comparison between subjective visual assessment and objective radiographic evaluation methods.

Key words: Carpal conformation; Carpal joint; Horses; Measurable parameters; Radiographs; Equine

1. INTRODUCTION

The conformation of the equine forelimb is very important to the overall athletic performance of the horse and its susceptibility to lameness as it bears over 55% of the horse's standing weight and is subjected to high compressional forces during galloping and landing phase of jumping (Clayton *et al.,* 2013; Kainer, 2002). The carpus must transmit large axial loads from the antebrachium to the distal forelimb and maintain optimum structural stability if the horse is to meet the heavy demand of

training, racing, and other athletic performances (Stashak & Hill, 2002). This stability is largely dependent on the conformation of the carpal bony structures.

Although some radiographic parameters have previously been developed to assess carpal conformation in horses; only few parameters are however regularly utilized. These include measuring "carpal angle" from both the dorsopalmar (DPa) and lateromedial (LM) radiographs (Barr, 1994; Fretz 1980); which the current authors have termed "medial carpal angle (MCA) and dorsal carpal angle (DCA) respectively to eliminate confusion in their description and orientation. In 2011, Abdunnabi developed 37 parameters from DPa radiographs and proposed their use in the conformational assessment of the equine carpus (Abdunnabi, 2011; Oheida *et al.,* 2016). Although, in contrast to previous studies (Barr, 1994; Fretz 1980), Abdunnabi (2011) validated the repeatability and reproducibility of specific landmarks used in developing the 37 DPa parameters, however the complexity involved in measuring most of these 37 parameters might make them unsuitable for routine/practical use. These complexities added to the shortcomings of objective carpal evaluation and may partly explained why only 10 out of the 37 parameters were published (Oheida *et al.,* 2016).

The equine carpal bones are classified as short bones (Getty, 1975) and have also been described as wedge-like in shape with topographic angulation of their articular surfaces (Bramlage, 1988; Deane & Davies, 1995a; Kainer, 2002; Von Rubeli, 1925). The carpal bones slide into a "close packed position" during weight bearing (a position where full congruities of all opposite and adjacent articular surfaces of the carpal bones occurred) and this unique morphology is believed to assist the carpus in attenuation of large axial forces by transferring some strain into the elastic intercarpal ligaments (Bramlage, 1988; Deane & Davies, 1995a; Von Boening, 1981). None of the 37 parameters (Abdunnabi, 2011; Oheida *et al.,* 2016) fully considered the topography of the articular surfaces of the carpal bones. Further investigation of the anatomy of the carpal DPa radiographs might therefore produce more measurable parameters that could estimate the degree of wedge or steepness of slope of these articular surfaces.

It would be beneficial to develop parameters from both the dorsopalmar and lateromedial radiographs of the carpal joint that would measure both the morphological and alignment aspects of conformation. This would provide a more holistic assessment of the carpal conformation in horses and probable predictive indices for biomechanical function and pathology of carpal joints. These parameters should be easy to measure, have consistent landmarks, reliably measure carpal conformational features, and show good repeatability (reliability) and reproducibility within and between different observers. Intraclass correlation coefficient (ICC) measures the reliability or consistency of measurements between two or more observers and could also show the reproducibility of experimental method and or agreement between two or more repeated measurements and observers (Bobak et al., 2018; Koo & Li 2016; Liljequist et al., 2019). The aims of this pilot study were: i) to investigate the radiographic anatomy of the equine carpus and develop measurable parameters such as angles and ratios that could be used to objectively measure the conformation of the carpus, ii) to

describe a detailed radiographic method for the measurement of the identified parameters, iii) to investigate the consistency of the positions of landmarks used to establish these parameters and iv) to investigate the reliability of the measurement protocol (parameters) between observers.

2. MATERIALS AND METHODS

2.1. Development of radiographic measurement techniques

Study design: This was a pilot study designed to test measurement and data collection protocol.

Ethical animal research: Approval from the University of Melbourne Animal Ethics Committee was not required as specimen were collected from animals that had either died or were euthanized for reasons not related to the study.

Animals: 10 forelimbs (from 7 thoroughbreds) aged 7.2±2.6 years were collected from the post-mortem room of the Department of Veterinary Pathology, University of Melbourne, Australia, and a local knackery in Melbourne. All the horses had either died or were euthanized for conditions not related to carpal injuries or lameness and owners' consent to use cadavers was obtained. The limbs were transected at about the midshaft of the antebrachium, wrapped in plastic bags, and preserved by freezing at -20°C until needed. Only limbs with carpi that had no visible physical injury and no radiographic abnormalities were included in the study.

Limb preparation and radiography: The limbs were defrosted in a chiller (5°C) for about 72 hours. Thereafter, each limb was mounted in a standing position on a customised loading rig (Alrtib, 2013) (Figure 1) and radiographed through lateromedial and dorsopalmar views using a portable radiographic machine (Atomscope HF80/15 UltraLight, Mikasa X-ray Co Ltd, Japan) set at 80 KVp and 24 secs (3.6 mAs). A common practice in our research group: Functional Anatomy and Biomechanics Laboratory (FABLAB), University of Melbourne, adopted for equine field radiography is to acquire images of the left limb in the lateromedial view and the right limb in the mediolateral position. This minimizes disturbance to the horses and reduces operational time per animal. A set of two lateral radiographs (i.e. lateromedial and mediolateral views) were therefore acquired for each of the 10 cadaveric limbs for comparison of carpal measurements on both lateral images.

2.1.1. Zero lateromedial/mediolateral (ZLM/ZML) carpal image

A specific rotational (oblique) image of the lateromedial view of the carpus, where the second and fourth metacarpal bones completely overlap, was acquired by slightly rotating the limb until the desired image was produced. This specific carpal image was defined as the "zero lateromedial" (ZLM) image (Figure 2a) produced from a "zero lateromedial" (ZLM) view or position. All carpal parameters were thereafter developed, measured, and compared on both zero lateromedial "ZLM" and zero mediolateral "ZML" images/views.

2.1.2. Zero dorsopalmar (ZDP) carpal View/image

The zero dorsopalmar (ZDP) view or image was defined as a dorsopalmar (DPa) view of the carpus at which its rotations along the vertical and horizontal axes were at zero degrees (Figure 2b)

(Abdunnabi, 2011; Oheida *et al.,* 2016). A straight line drawn to represent the proximal edge of the metacarpus and referred to as the reference line (RL) was previously established by Abdunnabi (2011) and reported to be parallel with the ground (Abdunnabi, 2011; Oheida *et al.,* 2016). These 2 previously established specific profiles of the DPa view (i.e ZDP and RL) were adopted for this study (Figure 2b).

The wedge angles of intermediate carpal bone (Ci) and the fourth carpal bone (C4) were measured directly from the radiographs while the slopes of the articular facets of the third (C3), radial (Cr) and ulnar (Cu) carpal bones were respectively used to calculate the respective slope angles for the C3, Cr and Cu. Geometrically, a wedge is a type of polyhedron (triangular prism) usually defined by two right angle triangles and three trapezoid faces. Using the principle of the right-angle triangle to relate to the "wedge-like" morphology of the carpal bones, if a long enough line (slope line) is drawn from the point of the wedge slope of each carpal bone facet (e.g. Cr and C3), it will eventually meet the continuation of the RL, and the angle thus formed would be termed the slope angle (x°) of that particular carpal bone facet (Figure 3). Another line drawn perpendicularly from any position on the RL to meet the wedge slope line will form another angle (y°). If angle y° was measured and then added to the known constant (90°) of right-angle triangles; then, the summation of y° and 90° could then be subtracted from 180° to get x° [i.e. $x = 180 - (90+y)$]. A parallel line to the RL on any transverse plane could be drawn to form the base of the right-angle triangle for each carpal bone wedge angle as required.

2.2. Radiographic measurement of carpal parameters

Selection of radiographs and development of measuring parameters (angles and ratios) were carried out by observer 1. Measurement and data recording were carried out on separate occasions by observer 1 and 2 at intervals of not less than 2 weeks from each set of measurements. All radiographic images were processed by Veterinary-80 CR Scanner (3D Imaging & Simulations Corp., Yuseong-Gu, Daejeon, Korea). Images were stored, analysed, and measured with an X-ray acquisition software (DICOM PACS® DX-R). All measurements were carried out with the same computer hardware (Dell® Latitude E6530). A summary of the abbreviations and meaning of some used technical details are provided in table 5 (the appendix). The following carpal parameters were developed to measure different aspects of carpal conformation.

2.2.1. Carpal parameters measurable on zero lateromedial/mediolateral (ZLM/ZML) radiographs

i. Dorsal carpal angle (DCA): was defined as the angle formed dorsally at the intersection of the long axis of the antebrachium and that of the third metacarpal bone. Although this angle was previously measured by Barr (1994), it was first termed/named DCA by Olusa (2018) and Olusa *et al.,* (2019). As shown in Figure 4a, the (dorsopalmar widths) of both the antebrachium and the metacarpus were each measured at 60mm and 120mm from the antebrachiocarpal and

carpometacarpal joints respectively and marked at the middle (midpoint) of these width. A straight line was then drawn through these marked midpoints of the bones to represent the long axis of both the antebrachium and the third metacarpus

ii. Distal radial slope carpal angle (DRSCA): was defined (Olusa, 2018; Olusa *et al.,* 2019) as the correlated angle formed by the disto-dorsal slope of the antebrachium as it articulates with the proximal row of the carpal bones (Figure 4b: ABD). Line "AB" was drawn as best fit from the most dorsal point of the rim of the distal radius through the distal epiphyseal slope of the radius, while line "BD" represented the dorsal height of Ci; from the distodorsal end (D) to its proximodorsal end (B).

iii. Intermediate carpal bone proximal tuberosity-radial angle (CiPxTRA): was measured as the angle formed from the highest point of the proximal articular surface (tuberosity) of Ci to the dorsal radial alignment (Figure 4b: ABC) (Olusa, 2018; Olusa *et al.,* 2019).

iv. Third carpal bone palmer facet angle (C3PalFCA): was measured as the angle formed between an extended line from the highest point of the proximal palmar articular surface of C3 (point E on Figure 4) to the disto-dorsal edge of the proximal carpal row alignment and a line (DB) representing the dorsal height of Ci (Figure 4b: EDB) (Olusa, 2018; Olusa *et al.,* 2019).

2.2.2. Carpal parameters measurable on zero dorsopalmar (ZDP) radiographs

i. Medial carpal angle (MCA): was the angle formed medially at the intersection of two lines drawn to represent the long axes of the radius and third metacarpal bones (Figure 4c) (Olusa, 2018; Olusa *et al.,* 2019).

ii. Disto-dorsal slope angle of the third carpal bone (C3DDSA): was the angle formed between the RL and the distal edge of C3 (Figure 5a: FEI). A line representing the distal edge of C3 (FE) was drawn from the most lateral end of the distal edge of C3 through to its most medial point and extended to meet the RL to form the slope angle ("x"). A second line was drawn perpendicularly from the RL to meet the line representing the distal edge of C3 (i.e FE) and the angle formed y° was measured and added to the constant 90° and then subtracted from 180° to get x°.

iii. Disto-dorsal slope angle of the radial carpal bone (CrDDSA): This was the angle formed between the RL and the dorsal aspect (slope) of the distal surface of Cr (Figure 5a: CD and Figure 5ai). A line "CD" drawn from the lateral margin of the disto-dorsal border of Cr (i.e the articulation point of Cr with C1 and C3), through to its medial edge and extended long enough until it meet the continuation of the RL represented the angle of the dorsal slope of the distal surface of Cr and was denoted by "x" (as shown in Figure 3). A perpendicular line from the RL was drawn to meet this distal slope line of Cr close to its lateral end to form the angle "y". The summation of "y" and 90° when subtracted from 180° produced "x".

iv. Proximo-dorsal slope angle of the radial carpal bone (CrPDSA): This was the angle formed between the RL and the dorsal aspect of the proximal surface of Cr. A line representing the dorsal slope of the proximal articular surface of Cr was drawn medially from the highest point of the proximal articular surface of Cr through to its medial edge (Figure 5a: AB and Figure 5ai). If "line

AB" was drawn long enough, it will eventually meet the continuation of the RL and form the proximo-dorsal slope angle of Cr (Cr PDSA) denoted by "x°". A second line was drawn perpendicularly from the RL to meet "line AB" at about its starting point to form angle "y" and was measured, added to 90° and then subtracted from 180° get "x" (Figures 3 and 5a: AB).

v. Distal slope angle of the ulnar carpal bone (CuDSA): This was the angle formed by a Cu distal topographic line "GH" drawn laterally from the medial edge of Cu articulation with Ci through to the lateral edge of Cu (Figure 5a: GH) and "extended" to meet the RL. It was similarly represented as "x" and calculated from [x = 180 - (90+y)] as previously described above.

vi. Disto-dorsal wedge angle of the intermediate carpal bone (CiDDWA): This was the angle formed at the dorsal articular ridge between the medial and lateral distal articular facets of Ci. A line "JK" was drawn laterally from the point of Ci articulation with Cr and the articular ridge between the radial and intermediate facets of C3 to the dorsal meeting point of Ci, C3 and C4 (Figure 5b: point "K") where it met with a second line "KL". The second line which represented the lateral articular facets of Ci was drawn medially from Ci articulation point with Cu extending to the Ci inter-facet articular ridge where it met with the first line to form CiDDWA (Figure 5b: JKL).

vii. Disto-dorsal wedge angle of the fourth carpal bone (C4DDWA): This was the angle formed at the articular ridge between the dorsal and lateral distal articular facets of C4. It was formed by 2 lines (Figure 5b and Figure 5bi: a' b' c'). The first line representing the dorsal articular facet of C4 (a′ b'), started from the distal meeting point of the images of C3 and C4 and extended to the articular ridge between the dorsal and lateral articular facets of C4. The second line (b' c') extended from this ridge to the lateral margin of the lateral articular facet of C4.

viii. Disto-palmar wedge angle of the fourth carpal bone (C4DPWA): This was the angle formed at the articular ridge between the palmar and lateral distal articular facets of C4 (Figure 5b and Figure 5bii: a b c'). It was represented by a line starting from medial margin of the palmar articular facet of C4 extending to the ridge (a b) and another line from the ridge extending to the lateral margin of the lateral articular facet of C4 (b c').

ix. Width ratio of distal radius to proximal metacarpus (WDR:WPM): This was the ratio of the width of the distal radius as measured from its most lateral to its most medial side (Figure 5c and Figure 5ci: AB) to the width of the proximal metacarpal bones as measured from the most lateral side of MC4 to the medial margin of MC2 (Figure 5c and Figure 5ci: CD).

x. Width ratio of distal radius' medial articular condyle to lateral articular condyle (DRW.MAC:LAC): This was the ratio of the width of medial articular condyle of the distal radius as measured from its medial margin to the inter-condylar ridge (Figure 5c and Figure 5cii: aH) to the width of the lateral articular condyle as measured from the inter-condylar ridge to its lateral margin Figure 5c and Figure 5cii: Hb).

2.3. Validation of consistency of position of landmarks for radiographic carpal parameters

After the initial set of radiographs were acquired, the limbs were then dissected to expose the carpal bones on both the dorsal and palmar aspects of the carpus and then radiographed a second time. A radiopaque material (flexible metal wire) was then cut and fixed with super glue to the anatomic features used as landmarks to develop the parameters and the limbs radiographed the third time. All the limbs were thus radiographed 3 times each at ZDP, ZLM and ZML views (i.e as intact limb before dissection; immediately after dissection and lastly after fixing the markers). The outline of the dorsal and palmar borders of each carpal bone was differentiated on the studied radiographs as explained in a standard radiographic anatomy text (Butler *et al.,* 2008).

2.4. Statistical analysis

All data were presented as Mean ± standard deviation (SD). One-way repeated measure ANOVA was used to compare means of each parameter measured from the three categories of carpal radiographs (i.e. from intact, dissected and metal marked). A paired Student t-test was used to compare the measurements from ZLM and ZML radiographs. Inter and intra observer reliability tests of measurements were analysed using paired t-test, intra class correlation coefficient (ICC) and Bland-Altman plot to chart the strength of agreement between the 2 independent observers. A Bland-Altman plot is chatted based on calculated mean difference of 2 separate measurements for the same variables and the upper and lower 95% limit of agreement. A 95% confidence interval was used and values where $P < 0.05$ were considered significant. All statistical tests were performed with MS Excel 2016 and Version 23 of IBM SPSS statistics for Windows.

3. RESULTS

14 parameters were developed from investigating the radiographic anatomy of the equine carpus. Four parameters were developed from the ZLM image (view) and 10 from the ZDP image (Table 1). No significant differences ($p > 0.05$) were observed between measurements obtained on the lateromedial (ZLM) and the mediolateral (ZML) images and between measurements of carpal parameters on radiographs from intact, dissected and metal marked limbs (Table 2). The differences between the repeated measurements of the two observers (Table 3) were not significantly different and the inter-observer ICC were generally good ranging from 0.581 to 0.969 (Table 4) except for WDR:WPM where the ICC was below 0.5 (0.443) and considered poor. A Bland-Altman plot showing the strength of agreement between the 2 observers was presented for each parameter (Figure 6a-n).

4. DISCUSSION

The data sets presented in this study for the 14 developed carpal parameters were generally well distributed except for CiPxTRA that was skewed to the left (Table 1). Graphically, the normality of a distribution (data set) is expressed by the dome shaped bell and it should appear symmetric if it looks the same to the left and to the right of the center point (Asghar & Zahediasl, 2012; Mishra et al., 2019). Skewness is the measure of lack of symmetry (i.e. asymmetry) of a normal distribution (data set). Ideally, for a symmetric distribution, the mean, median, and mode would coincide, and its skewness statistic = 0, but that hardly happens in most data set. Thus, distributions are considered

"approximate normal" if value is between −1 and +1 and considered highly skewed when less than -1 or greater than +1 (Asghar & Zahediasl, 2012; Mishra et al., 2019). A stricter value of between -0.5 and 0.5 for approximately symmetric, and between -1 and -0.5 or between 0.5 and 1 for moderately skewed is sometimes used for interpretation. It is difficult at this stage to ascertain the source or reason for the negative skewness of CiPxTRA observed in this study as it could either be a sample skewness without skewness in the population or an indication of skewness in the population.

The metal markers used in this study, made the landmarks used for the development of the parameters to be more visible (radiopaque) and thus reduced the chance of missing these points of interest. Measurements that were acquired with the aid of markers affixed to landmarks could therefore be regarded as true and accurate representations of distances or angles beteween two or more points of interest. Since there were no significant differences between measurements of the same parameters evaluated on radiographs from the marked and non marked preparations of same limb, it is reasonable to suggest that the measurements acquired without markers were as reliable as those with markers. This therefore validates that the location of the landmarks used on the radiographs were consistent and repeatable. The neccesity for verification of new methods suggests that measurement be taken more than once and also by more than one observer for comparison. Analysis of these repeated measures validate the consistency and repeatability of the method of measurement and the parameters been measured. The high intraclass correlation coefficient (ICC), found between and within measurements of the 2 observers in this study, thus further suggest clarity of parameters' landmarks and the ease and simplicity of the methodology.

Bland-Altman plot was introduced by Altman and Bland (1983) to describe the correlation or agreement more accurately between 2 quantitative measurements. It constructs on a scatter plot XY, the calculated mean difference (bias), and an upper and lower limit of agreement (LOA) between these 2 measurements. The Y axis shows the difference between the 2 paired measurements while the X axis represent the average of the 2 measurements (Giavarina, 2015). 95% of the data points are expected to be within ±2 standard deviation of the mean difference (centered line), represented by the 2 straight lines of upper and lower LOA respectively (Altman & Bland, 1983; Giavarina, 2015; Dogan, 2018). A strong inter-rater agreement observed in this study for all the 14 parameters could further affirm the accuracy, reliability, and reproducibility of measurements. Radiographic parameters were developed with the intent of measuring different aspects of the conformation of the equine carpus, so that when one or more parameters are evaluated together, a more comprehensive assessment of the carpus can be achieved.

The dorsal carpal angle (DCA) was developed to measure the general alignment of the carpus as viewed from the lateral aspect of the forelimb of the horse. Although the method used to measure DCA in this study was based primarily on the procedure described by Barr (1994), the term DCA was however not used in Barr's report. Other authors (Burn *et al.,* 2006; Deane & Davies, 1995b) have differently measured "carpal angle" also from the lateromedial view while still using the intersection

of the long axis of the antebrachium and the third metacarpal bone. They referred to the angle formed at the palmar aspect of the carpus as the "carpal angle". Confusion could therefore arise as to what orientation best defined the carpal angle or its proper nomenclature. The term DCA was therefore adopted in the current study to precisely identify the anatomical plane for which the angle has been measured. The term "hyperextension" is often used to describe overextending of a joint and carpal hyperextension has been reported to be associated with carpal damages and conformational unsoundness of the carpus in horses (Fretz, 1980; Barr, 1994; Deane & Davies, 1995b; Kainer, 2002; Stashak & Hill, 2002; Burn *et al.,* 2006). DCA measures the degree to which a carpus is either conformationally hyperextended (back-at-the-knee) or flexed ("Buck-kneed"). Also, during exercise, DCA could be used to either experimentally (Olusa *et al.,* 2019) or physiologically (Burn *et al.,* 2006; Deane & Davies, 1995b) assess the severity (degree) of hyperextension of the carpus at loading phase of locomotion.

The third carpal bone palmar facet angle (C3PalFCA) was conceived to measure the alignment of the middle carpal joint. Since the C3 palmar facet is a feature within the middle carpal joint, it was thought that the angle formed by its relative height with the dorsal margin of the proximal row of carpal bones, might affect either the forward or backward tilt of the proximal row of carpal bones, the distal antebrachium during loading and subsequently the entire carpal conformation. The middle carpal joint is a frequently damaged joint therefore, any parameter that can be used to assess its alignment (hyperextension) might be useful in diagnosis of middle carpal joint injuries and understanding of their pathogenesis. In a recent study, C3PalFCA was found useful for assessing the degree (severity) of carpal hyperextension as its values increase with increasing loading of the carpus (Olusa *et al.,* 2019). It also gave a more holistic evaluation of the carpus when assessed along with DCA as it was found to be inversely related to DCA (Olusa *et al.,* 2019).

The distal radial slope carpal angle (DRSCA) was designed to measure the conformational alignment of the disto-dorsal portion of the antebrachium (epiphysis) with the proximal row of carpal bones while the intermediate carpal bone proximal tuberosity-radial angle (CiPxTRA) attempts to assess the angular alignment formed between the highest point of the proximal row of carpal bones (the palmar tuberosity of Ci) and the disto-dorsal rim and epiphyseal slope of the radius. The palmar tuberosity of Ci has been reported to be more developed in the thoroughbred than in the pony (Abdunnabi *et al.,* 2011). CiPxTRA might therefore be helpful in further assessment of the degree of carpal hyperextension as it relates to or originates from the antebrachiocarpal joint.

The term "medial carpal angle" (MCA) has not been previously used to describe the measurement of "carpal angle" from the frontal plane of live horses, or on photographs of horses and on DPa radiographs. Nevertheless, the use of the intersection or pivot point of the radius and the third metacarpal bone has long been used in the horse especially when assessing the severity of angular limb deformities in foals (Butler, 2008; Fretz, 1980; Steinman *et al.,* 2000). MCA purpose was to measure the general alignment of the forelimb at the level of the carpus as viewed in the frontal plane.

This can be used routinely/clinically to objectively quantify the degree of carpal valgus or varus in the horse instead of the subjective method of dropping an imaginary line from the point of the shoulder joint to bisect the limb (Stashak & Hill, 2002). It will also be useful in assessing the degree of extension or hyperextension during loading and flexion of the carpus (Olusa *et al.,* 2019).

The current study measured for the first time the wedge-like angulations of the articular surfaces of the equine carpal bones. Although the interlocking wedge concept of the carpal bones have been described (Bramlage, 1988; Deane & Davies, 1995a; Rooney, 1969; Von Rubeli, 1925) there are no published measurements of these angles. Quantifying the topographic geometry of each carpal bone articular surfaces (Sledge, 1993), may however open a new area of investigation into how the biomechanics of the smooth load transmission from bone to ligament has protected the carpus from injury during the evolution of the horse.

The C3DDSA measures the angulation of the distal articular surface of C3. Since C3 is subjected to high compressional forces during loading (Bramlage, 1988; Palmer, 1994; Young et al., 1991), the steepness of this angle might have a possible correlation with how the C3 is conformationally stable on the MC3 during loading. In a study carried out by Abdunnabi (2011), out of 5 parameters that were used to categorize two limbs into "favourable" or "less favourable" carpal conformation and used to assess their stability under loading, 3 were related to the C3 (Abdunnabi, 2011). Other parameters related to C3 that were developed in the current study were CrDDSA and CiDDWA. The CrDDSA measures the steepness of the radial articular facet of C3 while CiDDWA partly measures the steepness of the intermediate articular facet of C3. The clinical extent of congruity maintained by Cr and Ci on C3 and on the proximal metacarpus by C3 during loading would be based on the degree of steepness and wedgeness of their articular surfaces and facets. Measuring the shape and geometrical properties of C3 might therefore provide a useful tool for quantifying the contributory role of C3 to the stability of the carpal joint in horses.

The wedge-like angulations of the distal surface of C4 promote its stability in-between the lateral splint bone, the third metacarpal bone and the C3 during loading. The steepness of these wedge-like angles of C3 and C4 could have important roles in the conformational stability of the distal carpal row which would be essential to the integrity of the carpometacarpal joint. On its proximal articular surface, the C4 articulates with the distal articular surface of ulnar carpal bone (Cu) during loading and thus CuDSA attempts to estimates the degree of congruity between the opposing surfaces of Cu and C4 under load.

The unique morphology of Ci has positioned it as the prime example of the wedge concept (Bramlage, 1988; Deane & Davies, 1995a; Rooney, 1969) and a clear depiction of the wedge-like angulation of the articular surfaces of the carpal bones (Bramlage, 1988). CiDDWA was conceived to measure the conformational stability of the Ci as it stabilizes/wedges between the C3 and C4 during weight bearing. The presence and degree of this angle might have an important role in the transfer of axial forces to the intercarpal ligaments between these bones. Auer et al., (1986) suggested that

spinning (rotational) movements occur around the long axes of the antebrachium and MC3 as the carpus is moving into a close-packed position during loading and that fractures of C4 and Ci are due to abnormal concentration of forces on these 2 bones. If the radius is rotating outward from medial to lateral (supination), while the MC3 is stationary or rotating lateromedially (i.e. inwardly and termed pronation), C4 and Ci are believed to be slammed together before other carpal bones can make full contact (Auer *et al.,* 1986). A steeper CiDDWA might therefore increase the slamming rate and impact of collision between these bones and result in increased incidence and severity of damage. Being able to measure this angle and ultimately establishing a safe value range for conformationally stable Ci may further help our understanding of loading, load transfer to adjacent bones and ligaments and pathogenesis of middle carpal joint damage.

Both the proximal and distal articular surface slope angles of Cr were measured. These measurements assess the degree of congruity of the proximal surface of the Cr with the radius and the distal surface of the Cr with the C3. The Cr is perhaps the most mobile of the carpal bones and receives high loading stress during flexion and extension of the antebrachiocarpal and middle carpal joints. A suggested mechanism of injury to these joints was repeated carpal hyperextension and resultant shortening (weakening) or microanatomic fractures of articular surfaces due to the chronic accumulation of loading stress (Bramlage, 1988). A deformed (weakened) articular surface may perhaps be measurable by assessing changes in the wedge angles. Furthermore, an increase or decrease in the steepness of these angles (CrDDSA and CrPDSA) might affect the loading stability of the Cr as it wedges in between the radius and the C3.

The width of the distal antebrachium would represent the proximal boundary of the carpus while the width of the metacarpus would represent the distal perimeter of the carpus. These 2 boundaries were measured as a ratio of each other (WDR:WPM). If a large difference exists between these 2 surfaces/width, it might result in a "funnel effect" in which a load travelling from the antebrachium will exert more pressure (strain) on the metacarpus due to the smaller recipient contact area. More studies will be required to test this theory.

DRW.MAC:LAC measures the relative width of the distal radius condyles. In another study, a similar measurement of widths of the lateral and the medial condyles of the distal extremity of MC3 showed that the medial condyle width was significantly larger than the lateral condyle (Alrtib *et al.,* 2012). This was thought to partly prevent the sliding of the proximal phalanx towards the lateral direction; a reason believed to be associated with the low incidence of fetlock luxation in horses (Alrtib *et al.,* 2012; Bertone, 2002). In the present study, the width of the medial articular condyle (MAC) of the distal radius was consistently less than the width of the lateral articular condyle (LAC). This would contribute to the conformational stability of the radius on the proximal carpal row as well as the general carpal alignment.

5. CONCLUSION

This study developed a radiographic measurement protocol and proposed 14 parameters for objective assessment of carpal conformation in the horse. These parameters are more holistic and yet simple to measure in comparison to previous methods. 5 of these 14 parameters were already found useful/relevant for assessing carpal conformation during experimental loading and flexion of the carpus (Olusa *et al.,* 2019). This evaluation protocol can be easily incorporated into routine radiographic examination of the horse such as pre purchase examination. With further studies on larger equine populations, and establishment of ranges of normal values for these parameters in different breeds, this technique offers a potential tool for clinicians for assessing different angular limb (carpal) conformation and physiological hyperextension in horses. This approach when adopted could also help to eliminate the often-encountered judgemental errors or variation between equine practitioners using subjective visual assessment for the carpus. Further investigation will be required for comparison between subjective visual examination and objective radiographic assessment methods of carpal conformation.

ACKNOWLEDGEMENT

The study was supported by Melbourne International Research Scholarship (MIRS) from The University of Melbourne, Australia. The authors would like to thank Brendan Kehoe and Dave Hobbs for assistance with samples collection and storage. Also, the expertise and input of Professor Ian Gordon, Director of Statistical Consulting Centre, University of Melbourne for assistance/consultation about choice of statistical tests, study design and analysis was duly acknowledged.

CONFLICT OF INTEREST

No conflict of interest is declared for this work.

DATA AVAILABILITY STATEMENT

The data that support the findings of this study are available from the corresponding author upon request.

FUNDING

The study was supported by Melbourne International Research Scholarship (MIRS) from The University of Melbourne, Australia.

REFERENCES

Abdunnabi, A.H. (2011). Morphometry of the equine carpus and its relationship to carpal bone pathology. University of Melbourne (PhD Thesis), Victoria, Australia.

Abdunnabi, A.H., Ahmed, A.Y., Philip, C.J., & Davies, H.M.S. (2011). Morphological variations of carpal bones in thoroughbreds and ponies. *Anatomia histologia embryologia, 41, 139-148.*

Alrtib, A.M. (2013). Radiographic bone morphometry of the equine metacarpophalangeal joint and relationships to the incidence of pathology in thoroughbred racehorses. University of Melbourne (PhD Thesis), Victoria, Australia.

Alrtib, A.M., Philip, C.J., Abdunnabi, A.H., & Davies, H.M.S. (2012). Morphometrical study of bony elements of the forelimb fetlock joint in horses. *Anatomia histologia embryologia*. DOI: 10.1111/j.1439-0264.2012.01158.x Altman, D.G., Bland, J.M. (1983). Measurement in medicine: the analysis of method comparison studies. *Statistician, 32:307–17.* http://dx.doi.org/10.2307/2987937.

Auer, J.A., Watkins, J.P., White, N.A., Taylor, T.S., & Rooney, J.R. (1986). Slab fractures of the fourth and intermediate carpal bones in five horses. *Journal of American Veterinary Medical Association, 188, 592-601.*

Barr, A.R.S. (1994). Carpal conformation in relation to carpal chip fracture. *Veterinary Record, 134, 646-650.*

Bertone, A.L. (2002). Lameness: Adam's Lameness in Horses (5th ed.), Stashak, T.S. editor. USA: Lippincott Williams & Wilkins Philadelphia. p. 790.

Bobak, C.A., Barr, P.J., & O'Malley, A.J. (2018). Estimation of an inter-rater intra-class correlation coefficient that overcomes common assumption violations in the assessment of health measurement scales. *BMC medical research methodology, 18, 93.* doi.org/10.1186/s12874-018-0550-6

Bramlage, L.R., Schneider, R.K., & Gabel, A.A. (1988). A clinical perspective on lameness originating from the carpus*. Equine veterinary journal, Suppl 6, 12-18.*

Burn, J.F., Portus, B., & Brockington, C. (2006). The effect of speed and gradient on hyperextension of the equine carpus. *The veterinary journal, 171, 169-171.*

Butler, J.A., Colles, C.M., Dyson, S.J., & Poulos, P.W. (2008). The carpus and antebrachium: Clinical Radiology of the horse (3rd ed.), UK: Wiley-Blackwell. p 33-271.

Clayton, H.M., Chateau, H., & Back W. (2013). Forelimb function: Equine Locomotion (2nd ed.), Back, W., & Clayton, H.M. editors. Saunders Elsevier, p 99-125.

Deane, N.J., & Davies, A.S. (1995a). The function of the equine carpal joint: A review. *New Zealand veterinary journal, 43, 45-47.*

Deane, N.J., & Davies, A.S. (1995b). A preliminary study of hyperextension of the carpal joint in the racing thoroughbred. *New Zealand veterinary journal, 43, 83-84.*Dogan, N.O. (2018). Bland-Altman analysis: A paradigm to understand correlation and agreement. *Turkish Journal of Emergency Medicine, 18, 139–141* https://doi.org/10.1016/j.tjem.2018.09.001

retz, P.B. (1980). Angular limb deformities in foals. *Veterinary Clinic of North America Large Animal Practice, 2, 125-150.*

Getty, R.S. (1975). Osteology of the horse: Sisson and Grossman's The Anatomy of Domestic Animals (5th ed.) Philadelphia: Saunders WB. p 357.

Ghasemi, A., & Zahediasl, S. (2012). Normality tests for statistical analysis: a guide for non-statisticians. *International journal of endocrinology and metabolism*, *10*(2), 486–489. https://doi.org/10.5812/ijem.3505

Giavarina, D. (2015). Understanding Bland Altman analysis. *Biochemia medica*, *25*(2), 141–151. https://doi.org/10.11613/BM.2015.015

Kainer, R.A. (2002). Functional anatomy of the equine locomotor organs: Adam's Lameness in Horses (5th ed.) Stashak, T. editor. Philadelphia, USA: Lippincott Williams & Wilkins. p 1-72.

Koo, T.K., & Li, M.Y. (2016). A guideline of selecting and reporting intraclass correlation coefficients for reliability research. *Journal of Chiropractic Medicine, 15, 155–163.* doi.org/10.1016/j.jcm.2016.02.012

Liljequist, D., Elfving, B., & Skavberg Roaldsen, K. (2019). Intraclass correlation – A discussion and demonstration of basic features. PLOS ONE 14 (7), e0219854. doi.org/10.1371/journal.pone.0219854

Mishra, P., Pandey, C. M., Singh, U., Gupta, A., Sahu, C., & Keshri, A. (2019). Descriptive statistics and normality tests for statistical data. *Annals of cardiac anaesthesia*, *22*(1), 67–72. https://doi.org/10.4103/aca.ACA_157_18

Oheida, A.H., Anderson, G.A., Alrtib, A.M., Abushhiwa, M.H., Philips, C.J., & Davies, H.M.S. (2016). Carpal parameters on dorsopalmar radiographs of the equine carpus. *Journal of veterinary advances, 6, 1258-1268.*

Olusa, T.A.O. (2018). Radiographic assessment of bone morphometry, alignment and loading stability of the equine carpal joint in racehorses. University of Melbourne (PhD Thesis), Victoria, Australia.

Olusa, T.A.O., Murray, C.M., & Davies, H.M.S. (2019). Radiographic assessment of the equine carpal joint under incremental loads and during flexion. *Comparative Exercise Physiology,* 1 – 12. doi.org/10.3920/CEP180044

Palmer, J.L., Bertone, A.L., Litsky, A.S. (1994). Contact area and pressure distribution changes of the equine third carpal bone during loading. *Equine veterinary journal, 26, 197-202.*

Rooney, J.R. (1969). Biomechanics of lameness in horses. Baltimore: Williams and Wilkins.

Sledge, C.B. (1993). Biology of the joint: Textbook of Rheumatology (4th ed.) Kelley, W.N., Harris, E.D., Ruddy, S., & Sledge, C.B. Editors. Philadelphia: Saunders WB. p 1-21.

Stashak, T.S., & Hill, C. (2002). Conformation and movement: Adam's Lameness in Horses (5th ed.) Stashak, T.S. editor. Philadelphia, USA: Lippincott Williams & Wilkins. p 73-111.

Steinman, A., Klemer, G., Levi, O., Avni, G., & Singer, E.R. (2000). Congenital angular limb deformity of the carpus in a foal: a report of a complicated case and review of literature. *Israel journal of veterinary medicine, 55, 22-24.*

Von Boening, K.J. (1981). Hyperextension folgen im Karpalgelenks bereich. *Der praktische Tierarzt, 7, 606- 608.*

Von Rubeli, O. (1925). Zur Anatomie und Mechanik des Karpalgelenks der Haustiere, Speziell des Pferdes. *Schweizer Archiv fiir Tierheilkunde, 67, 427-432.*

Young, D.R., Richardson, D.W., Markel, M.D., & Nunamaker, D.M. (1991). Mechanical and morphometric analysis of the third carpal bone of thoroughbreds. *American journal of veterinary research, 52, 402-409.*

Table 1: 14 Carpal conformational parameters measured from Zero lateromedial (ZLM) and Zero dorsopalmar (ZDP) radiographs of 10 cadaveric limbs

S/no	Measurable Parameters (n=10)	Mean ± SD (°)	Median (°)	95% C I of Mean		Skewness Statistic
				Lower	Upper	
1	**DCA**	176.61±0.66	176.79	176.14	177.08	-0.529
2	**DRSCA**	145.59±2.19	145.65	144.02	147.15	0.607
3	**CiPxTRA**	115.69±3.15	117.24	113.44	117.94	-1.495**
4	**C3PalFCA**	84.43±1.13	84.48	83.62	85.24	-0.502
5	**MCA**	183.34±1.02	183.49	182.61	184.07	-0.314
6	**C3DDSA**	8.27±0.92	8.21	7.61	8.93	0.638
7	**C4DDWA**	141.71±2.85	140.71	139.67	143.75	0.657
8	**C4DPWA**	128.31±5.03	129.67	124.72	131.91	-0.219
9	**CrDDSA**	7.91±1.16	8.07	7.08	8.74	0.249
10	**CrPDSA**	13.44±0.87	13.48	12.81	14.06	-0.077
11	**CiDDWA**	153.08±2.19	153.39	151.52	154.64	-0.368
12	**CuDSA**	33.02±2.77	32.44	31.04	35.01	0.649
13	**WDR: WPM**	1.13±.03	1.13	1.11	1.15	0.583
14	**DRW.MAC:LAC**	0.77±0.06	0.79	0.72	0.81	-0.244

DCA = Dorsal carpal angle; **DRSCA** = Distal radial slope carpal angle; **CiPxTRA =** Intermediate carpal bone proximal tuberosity-radial angle; **C3PalFCA = t**hird carpal bone palmer facet angle; **MCA** = Medial carpal angle; **C3DDSA** = Disto-dorsal slope angle of the third carpal bone; **C4DDWA** = Disto-dorsal wedge angle of the fourth carpal bone; **C4DPWA** = Disto-palmar wedge angle of the fourth carpal bone; **CrDDSA** = Disto-dorsal slope angle of the radial carpal bone; **CrPDSA** = Proximo-dorsal slope angle of the radial carpal bone; **CiDDWA** = Disto-dorsal wedge angle of the intermediate carpal bone; **CuDSA** = Distal slope angle of the ulnar carpal bone; **WDR:WPM** = Width ratio of distal radius to proximal metacarpus; **DRW.MAC:LAC** = Width ratio of distal radius' medial articular condyle to lateral articular condyle. **95% C I** = 95% Confidence interval; **(°)** = Degrees. The unit of measurement was in degree for all the parameters except for WDR:WPM and DRW.MAC:LAC that are ratios and had no unit. **SD** = Standard deviation. btw = between. ****** = highly skewed

Skewness statistic measures lack of symmetry (asymmetry) of normal distribution of a data set. perfect symmetric = 0; approximate normal/symmetric = btw -0.5 and 0.5; moderately skewed = btw -1 and -0.5 or 0.5 and 1; and highly skewed = less than -1 or greater than 1.

Table 2: Validation of the consistency of the positions of landmarks used for measuring the 14 carpal parameters from ZLM and ZDP radiographs

S/no	Measurable Parameters (n = 10)		Mean ± SD (°)						Sig. btw int, dis & mak carpi (p<0.05)*
			Intact limb/ Carpi	Sig. (p value) btw ZLM & ZML	Dissected limb/ Carpi	Sig. (p value) btw ZLM & ZML	Carpi with marker	Sig. (p value) btw ZLM & ZML	
1	**DCA**	**ZLM**	176.61±0.66	0.273	176.45±0.81	0.265	176.88±0.62	0.286	**0.403**
		ZML	176.25±0.50		176.79±0.48		176.46±0.77		
2	**DRSCA**	**ZLM**	145.59±2.19	0.789	144.89±1.73	0.643	145.22±1.81	0.828	**0.725**
		ZML	145.87±2.09		144.61±1.69		145.07±1.68		
3	**CiPxTRA**	**ZLM**	115.69±3.15	0.981	114.82±1.91	0.582	115.93±2.49	0.850	**0.602**
		ZML	115.72±2.01		115.47±2.33		115.79±1.95		
4	**C3PalFCA**	**ZLM**	84.43±1.13	0.574	84.71±1.95	0.924	85.26±2.03	0.709	**0.567**

	ZML	84.81±1.66		84.78±1.85		84.95±1.58		
5	**MCA**	183.34±1.02	na	183.99±1.33	na	183.89±1.36	na	**0.463**
6	**C3DDSA**	8.27±0.92	na	8.02±0.81	na	8.08±0.90	na	**0.807**
7	**C4DDWA**	141.71±2.85	na	141.24±3.00	na	142.17±3.21	na	**0.791**
8	**C4DPWA**	128.31±5.03	na	128.18±4.09	na	128.22±5.68	na	**0.998**
9	**CrDDSA**	7.91±1.16	na	7.64±0.88	na	8.16±1.01	na	**0.536**
10	**CrPDSA**	13.44±0.87	na	13.45±1.36	na	13.52±1.82	na	**0.990**
11	**CiDDWA**	153.08±2.19	na	151.62±2.76	na	153.63±3.11	na	**0.250**
12	**CuDSA**	33.02±2.77	na	33.19±3.00	na	35.05±3.27	na	**0.269**
13	**WDR:WPM**	1.13±.03	na	1.13±0.02	na	1.13±0.03	na	**0.821**
14	**DRW.MAC:LAC**	0.77±0.06	na	0.78±0.04	na	0.77±0.06	na	**0.828**

DCA = Dorsal Carpal Angle; **DRSCA** = Distal Radial Slope Carpal angle; **CiPxTRA =** Intermediate carpal bone Proximal Tuberosity-Radial Angle; **C3PalFCA =** Third carpal bone Palmer facet angle; **MCA** = Medial Carpal angle; **C3DDSA** = Disto-dorsal slope angle of the third carpal bone; **C4DDWA** = Disto-dorsal wedge angle of the fourth carpal bone; **C4DPWA** = Disto-palmar wedge angle of the fourth carpal bone; **CrDDSA** = Disto-dorsal slope angle of the radial carpal bone; **CrPDSA** = Proximo-dorsal slope angle of the radial carpal bone; **CiDDWA** = Disto-dorsal wedge angle of the intermediate carpal bone; **CuDSA** = Distal slope angle of the ulnar carpal bone; **WDR:WPM** = Width ratio of Distal radius to Proximal metacarpus; **DRW.MAC:LAC** = Width ratio of distal radius' medial articular condyle to lateral articular condyle. **95% C I** = 95% Confidence interval; **SD** = Standard deviation; na = non applicable; btw = between; ***** = Statistical significance (**Sig.**) at **p<0.05. int = intact, dis = dissected, mak = marked.**

Table 3: Intra-observer repeatability (test re-test reliability) test for each of the 14 carpal parameters measured separately by 2 independent observers. Results showed no significant mean difference and intraclass correlation coefficient (ICC) between their (i.e. Obr 1 & 2) respective 2 repeated measurements.

S/ no	Parameters (n = 10)	Mst/ Reading	Observer 1				Observer 2			
			Mean±SD	Mean Diff.±SD	Sig. (p<0.05)*	ICC (95% CI)	Mean±SD	Mean Diff.±SD	Sig. (p<0.05)*	ICC (95% CI)
1	**DCA**	1st	176.61±0.66	0.20±0.64	0.344	0.616	176.52±0.60	-0.02±0.69	0.925	0.660

		2nd	176.41±0.56			(-0.464; 0.903)	176.54±0.72			(-0.542; 0.918)
2	**DRSCA**	1st	145.59±2.19	0.16±1.55	0.755	0.808	145.98±1.33	0.67±1.62	0.494	0.668
		2nd	145.43±1.47			(0.188; 0.953)	145.31±1.85			(-0.356; 0.918)
3	**CiPxTRA**	1st	115.69±3.15	0.07±0.92	0.811	0.975	116.55±1.29	0.32±0.81	0.244	0.895
		2nd	115.62±2.46			(0.899; 0.994)	116.24±1.39			(0.607; 0.974)
4	**C3PalFCA**	1st	84.43±1.13	0.09±1.09	0.785	0.744	84.57±1.85	-0.18±1.78	0.759	0.620
		2nd	84.33±1.22			(-0.108; 0.938)	84.75±1.46			(-0.709; 0.908)
5	**MCA**	1st	183.34±1.02	-0.04±0.78	0.881	0.852	183.61±1.05	-0.42±0.73	0.867	0.753
		2nd	183.38±1.08			(0.379; 0.964)	184.03±0.94			(-2.799; 0.795)
6	**C3DDSA**	1st	8.27±0.92	-0.26±0.31	0.027	0.949	8.29±0.58	-0.09±0.55	0.624	0.852
		2nd	8.52±0.80			(0.670; 0.989)	8.38±0.88			(0.401; 0.963)
7	**C4DDWA**	1st	141.71±2.85	-0.39±1.08	0.280	0.951	142.41±2.39	-0.06±1.94	0.924	0.806
		2nd	142.10±2.15			(0.813; 0.988)	142.47±2.26			(0.166; 0.953)
8	**C4DPWA**	1st	128.31±5.03	-0.37±1.02	0.273	0.989	128.83±6.01	0.10±2.01	0.874	0.965
		2nd	128.69±5.09			(0.960; 0.997)	128.73±4.22			(0.856; 0.991)
9	**CrDDSA**	1st	7.91±1.16	-0.01±0.38	0.909	0.973	8.14±0.77	-0.08±0.59	0.664	0.846
		2nd	7.93±1.05			(0.891; 0.993)	8.22±0.80			(0.370; 0.962)
10	**CrPDSA**	1st	13.44±0.87	-0.15±0.91	0.606	0.845	13.23±1.25	-0.05±0.65	0.810	0.924
		2nd	13.59±1.48			(0.372; 0.962)	13.28±1.09			(0.688; 0.981)
11	**CiDDWA**	1st	153.08±2.19	0.27±0.91	0.379	0.957	153.24±1.96	0.44±0.73	0.093	0.963
		2nd	152.81±2.29			(0.838; 0.989)	152.80±2.35			(0.836; 0.991)
12	**CuDSA**	1st	33.02±2.77	0.36±0.63	0.099	0.985	32.62±2.63	0.18±0.71	0.447	0.982
		2nd	32.66±2.86			(0.931; 0.996)	32.44±2.56			(0.930; 0.995)
13	**WDR:WPM**	1st	1.13±0.03	-0.001±0.02	0.876	0.852	1.13±0.03	0.001±0.02	0.859	0.883
		2nd	1.13±0.02			(0.377; 0.964)	1.13±0.02			(0.512; 0.971)

14	**DRW.MAC: LAC**	1st	0.77±0.06	-0.008±0.04	0.534	0.866 (0.467; 0.966)	0.78±0.05	0.01±0.06	0.761	0.802 (0.404; 0.885)
		2nd	0.77±0.05				0.77±0.05			

Measurement (Mst) Reading refers to the separate 1st and 2nd time points (minimum of 2 weeks interval) of repeated measurement of radiographs by the two observers. **95% CI =** 95% Confidence interval. **Mean Diff** = Difference between 2 means. **SD** = Standard deviation. ***** = Statistical significance (**Sig.**) at **p<0.05**

Table 4: Assessment of agreement of measurement between the 2 independent observers (Inter-rater reliability test) for each of the 14 carpal parameters using calculated mean difference (bias) and 95% limit of agreement (CI) for the Bland-Altman plot

S/ no	Parameters	Observers	Mean±SD	Mean Diff.±SD	Sig (p<0.05)*	Intraclass Correlation Coefficient (95% CI)	Calc. 95% CI for Limits of agreement (for Bland-Altman plot)	
							Lower	Upper
1	**DCA**	1st	176.61±0.66	0.09±0.83	0.739	0.621 (-1.855; 0.922)	-1.5324	1.7124
		2nd	176.52±0.60					
2	**DRSCA**	1st	145.59±2.19	-0.39±0.97	0.844	0.823 (0.248; 0.957)	-2.3002	1.5142
		2nd	145.98±1.33					
3	**CiPxTRA**	1st	115.69±3.15	-0.86±2.81	0.257	0.884 (0.165; 0.987)	-6.3694	4.6454
		2nd	116.55±1.29					
4	**C3PalFCA**	1st	84.43±1.13	-0.14±2.03	0.735	0.732 (-0.174; 0.820)	-4.1168	3.8408
		2nd	84.57±1.45					
5	**MCA**	1st	183.34±1.02	-0.27±1.71	0.096	0.581 (-0.547; 0.834)	-3.6309	3.0829
		2nd	183.61±1.54					
6	**C3DDSA**	1st	8.27±0.92	-0.02±0.59	0.914	0.907 (0.307; 0.987)	-1.1939	1.1519
		2nd	8.29±0.58					
7	**C4DDWA**	1st	141.71±2.85	-0.70±1.52	0.177	0.922 (0.539; 0.989)	-3.6849	2.2769
		2nd	142.41±2.39					

8	**C4DPWA**	1st	128.31±5.03	-0.52±1.27	0.228	0.989 (0.895; 0.998)	-3.0054	1.9674
		2nd	128.83±6.01					
9	**CrDDSA**	1st	7.91±1.16	-0.22±0.55	0.228	0.916 (0.564; 0.987)	-1.3473	0.8993
		2nd	8.14±0.77					
10	**CrPDSA**	1st	13.44±0.87	0.20±0.99	0.532	0.789 (-0.269; 0.970)	-1.7406	2.1486
		2nd	13.23±1.25					
11	**CiDDWA**	1st	153.08±2.19	-0.16±1.42	0.731	0.969 (0.769; 0.995)	-2.9519	2.6319
		2nd	153.24±1.96					
12	**CuDSA**	1st	33.02±2.77	0.41±1.38	0.373	0.872 (0.861; 0.927)	-2.2888	3.1048
		2nd	32.62±2.63					
13	**WDR:WPM**	1st	1.13±0.03	-0.01±0.03	0.614	0.443 (-2.686; 0.883)	-0.0643	0.0543
		2nd	1.13±0.03					
14	**DRW.MAC:LAC**	1st	0.77±0.06	-0.01±0.05	0.521	0.869 (0.542; 0.989)	-0.1029	0.0829
		2nd	0.78±0.05					

Estimates of reliability based on ICC values are categorized as follows: below 0.5 = Poor; 0.5 to 0.75 = Moderate; 0.75 to 0.9 = Good and above 0.9 = Excellent (Koo & Li 2016). ***** = Statistical significance (**Sig.**) at **$p<0.05$**

Table 5: (Appendix) Abbreviations and details of technical parameters used for imaging

DP	**Dorsopalmar:** This refers to the direction of travel of the primary X-ray beam as viewed from the frontal plane of the horse/limb. The beam enters on the dorsal surface of the carpus and exit from the palmar side
LM	**Lateromedial:** This refers to the direction of travel of the primary X-ray beam as it enters on the lateral side of the limb and exit from the medial side

ML	**Mediolateral:** X-ray beam travelled in opposite direction to LM
ZDP	**Zero dorsopalmar:** This is an oblique variation of dorsopalmar view. It is usually obtained when the direction of travel of the primary X-ray beam entered the object at between 2° to 15° Dorsolateral-Palmaromedial Oblique (DL-PaMO). The angulation of the oblique depends on the conformation of each limb. The aim was to produce a radiograph of the carpus with i) a small radiolucent space between the proximo-dorsal articular facets of the radial carpal bone (Cr) and intermediate carpal bone (Ci); and ii) a contact point between the disto-lateral ends of the dorsal and the palmar borders of the third carpal bone (C3). These 2 features respectively served as the vertical and horizontal landmarks for ZDP view
ZLM	**Zero Lateromedial:** This was essentially a Palmarolateral-Dorsomedial Oblique (PaL-DMO) view. The oblique angle varied from between 5° to 20° depending on each limb's conformation. The aim of this view was to produce a radiograph in which the overlapped 4th and 2nd metacarpal bones were completely superimposed; represented by a single clear margin of their palmar borders
ZML	**Zero Mediolateral:** This was opposite to ZLM as the direction of travel of the primary X-ray beam was Dorsomedial-Palmarolateral Oblique (DM-PaLO) at similar angles
DICOM	Digital imaging and communication in medicine
PACS	Picture archiving and communication system

ahe_12627_f1.tif

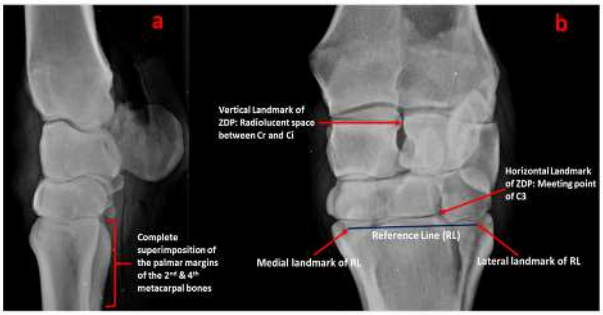

ahe_12627_f2.tif

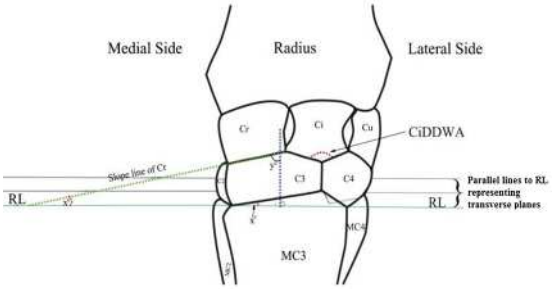

ahe_12627_f3.tif

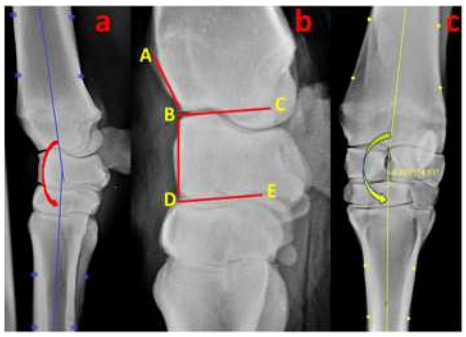

ahe_12627_f4.tif

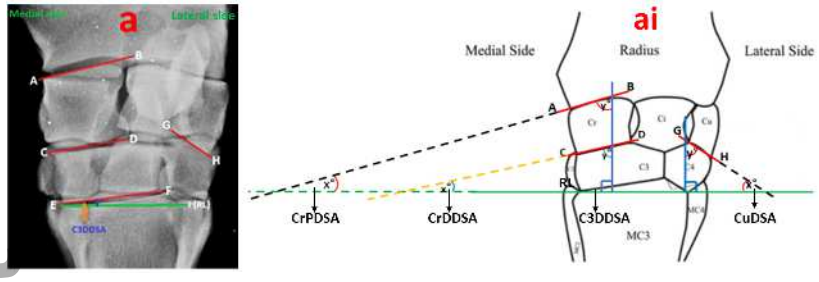

ahe_12627_f5a.tif

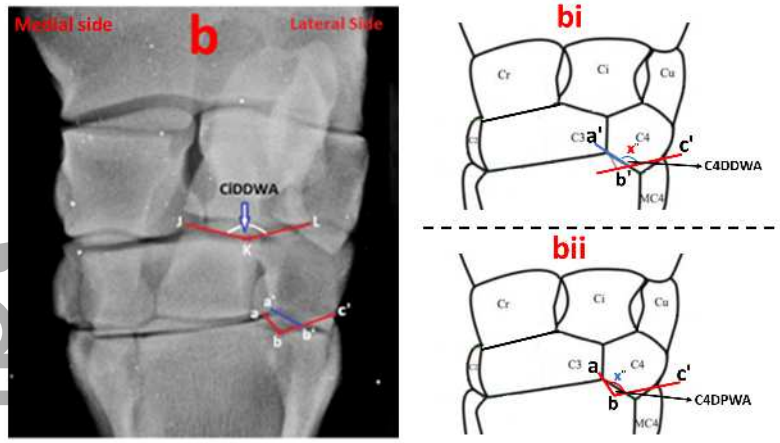

ahe_12627_f5b.tif

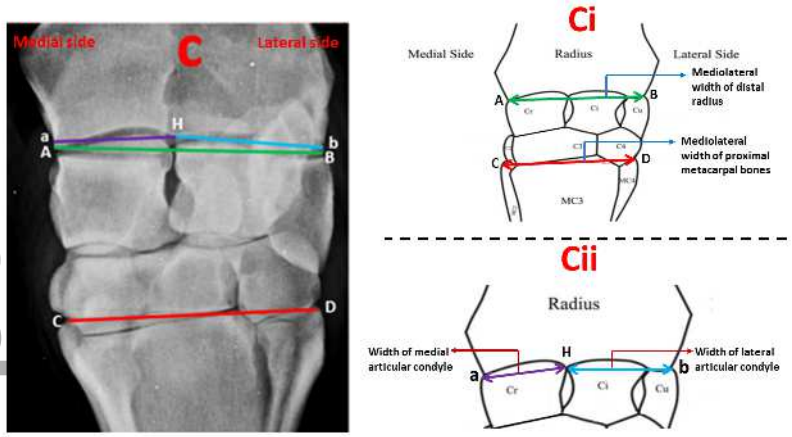

ahe_12627_f5c.tif

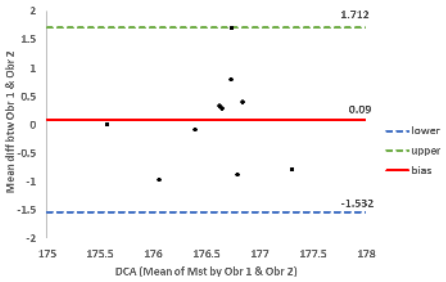

ahe_12627_f6a.tif

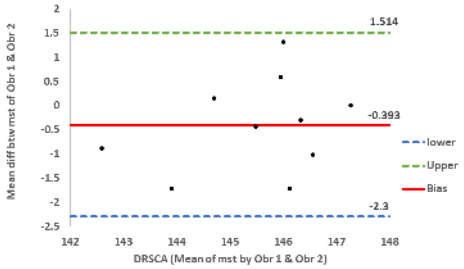

ahe_12627_f6b.tif

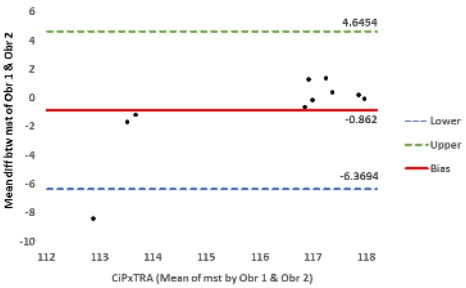

ahe_12627_f6c.tif

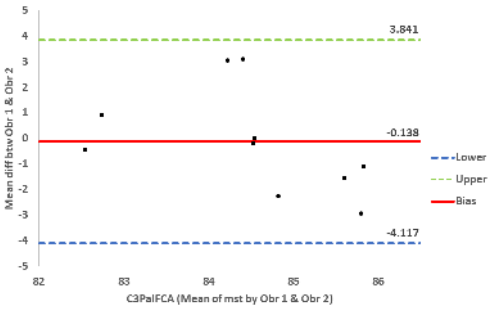

ahe_12627_f6d.tif

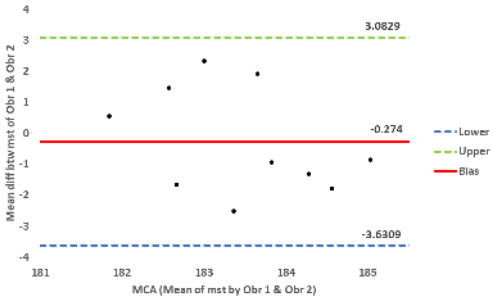

ahe_12627_f6e.tif

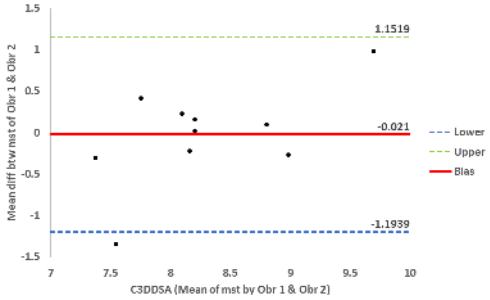

ahe_12627_f6f.tif

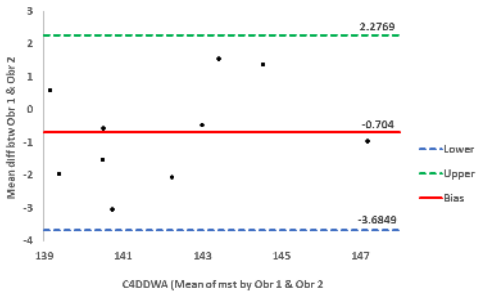

ahe_12627_f6g.tif

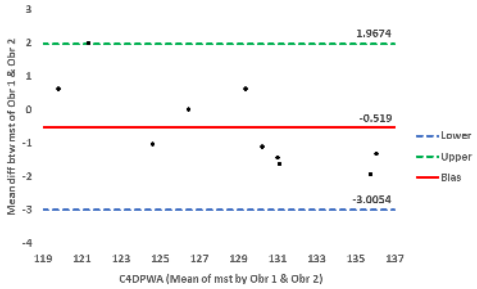

ahe_12627_f6h.tif

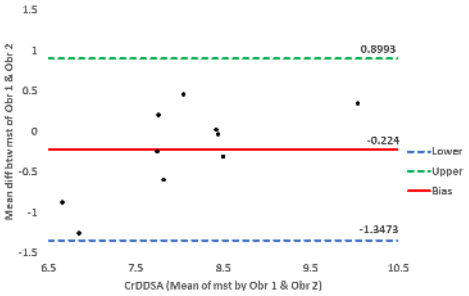

ahe_12627_f6i.tif

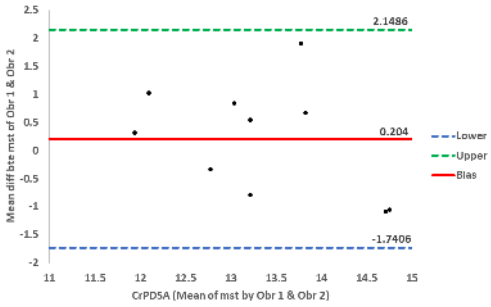

ahe_12627_f6j.tif

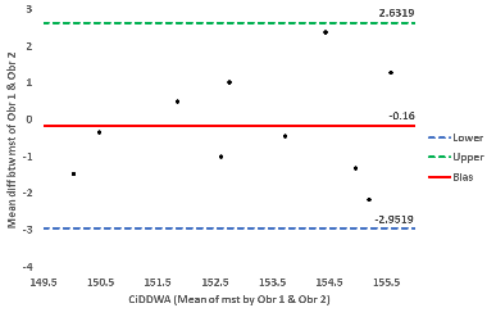

ahe_12627_f6k.tif

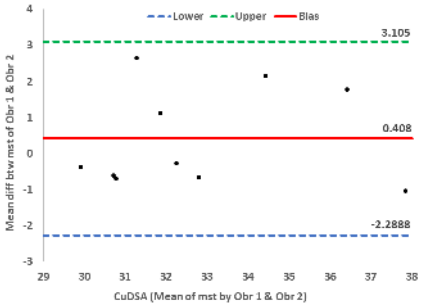

ahe_12627_f6l.tif

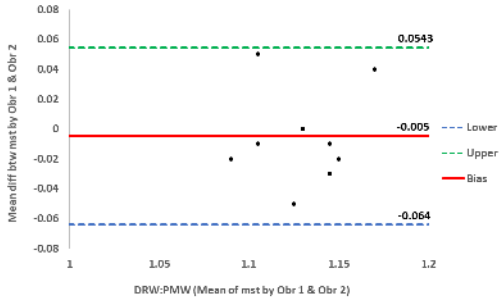

ahe_12627_f6m.tif

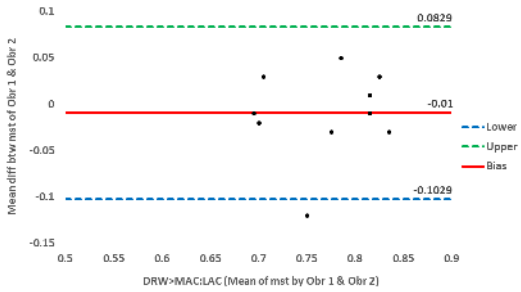

ahe_12627_f6n.tif